Lasers in Manufacturing Conference 2015

Laser beam propagation and energy deposition in particulate PEEK layers

Hendrik Sändker[a,*], Jochen Stollenwerk[a,b], Johannes Hofmann[a], Peter Loosen[a,b]

[a]*Fraunhofer Institute for Laser Technology ILT, Steinbachstr. 15, 52074 Aachen, Germany*
[b]*Chair for Technology of Optical Systems TOS, RWTH Aachen University, Steinbachstr. 15, 52074 Aachen, Germany*

Abstract

The usage of high-temperature resisting thermoplastic polymers like PEEK (polyether ether ketone) as coating material represents an alternative to conventional corrosion protection layers. One promising approach to manufacture these coatings is to deposit particulate PEEK and, subsequently, melt the PEEK particles by laser radiation in order to create a dense, pore-free layer. Understanding the laser beam propagation and the energy deposition in the particulate PEEK layer is essential to simulate (time-dependent) temperature distributions within the layer system. These simulations allow an efficient identification of suitable process parameters for laser melting of the PEEK layer. Therefore, the absorbance of the layer system composed of substrate and PEEK powder with admixed laser-absorbing particles is determined experimentally. Subsequently, a model-based simulation of the optical properties is conducted and fitted to the measured data. Hence, the complex refractive indices of the bulk materials, particle-size distribution, powder density, multiple reflection, various scattering effects as well as layer thickness are taken into account. Based on the simulation results the spatial energy deposition in the layer system is extracted.

Keywords: Surface Functionalization; Fundamentals and Process Simulation

1. Motivation

Sustainable anti-corrosion strategies are becoming increasingly important as energy and material consumption is growing globally. Particularly in the field of alternative generation of energy, such as wind

* Corresponding author. Tel.: +49 241 8906-361; Fax +49 241 8906-121.
E-mail address: hendrik.saendker@ilt.fraunhofer.de

power and solar thermal power, the construction of new plants often involves exploiting areas with a high corrosive potential. The usage of high-temperature resisting thermoplastic polymers like PEEK (polyether ether ketone) as coating material represents an alternative to conventional corrosion protection layers. Therefore, together with industrial partners, the Fraunhofer Institute for Laser Technology is investigating the laser-based production of polymer coatings for high precision components. The investigated process chain comprises four consecutive steps Fig. 1): the laser-based pre-treatment of the substrates (1), the preparation of a hydrous dispersion based on PEEK powder or preparation of powder blend (2), the deposition of the dispersion by knife coating or the deposition of the powder blend by spray coating (3), and the laser-based thermal post-treatment by means of melting the PEEK powder with IR-laser radiation (4). An outstanding challenge results from using temperature-sensitive bearing steel with annealing temperatures between 180°C and 200°C [1], hence below the melting temperature of PEEK of approximately 340°C [2].

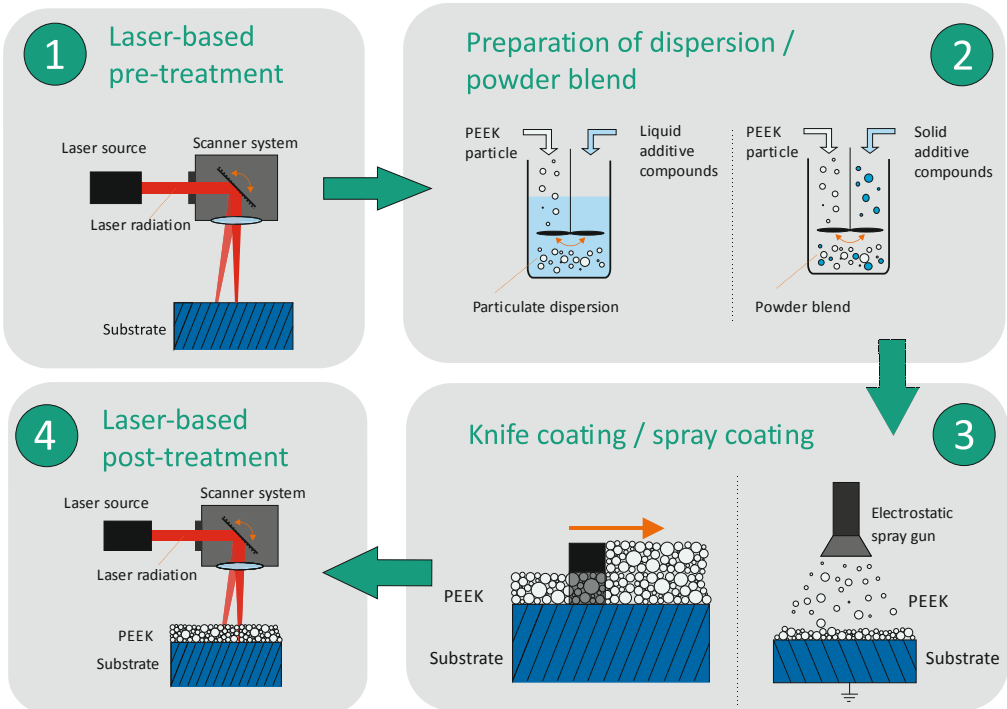

Fig. 1.: Overview of the investigated process chain.

For understanding the laser melting (post-treatment) process it is necessary to know how the laser beam propagates through the particulate PEEK powder and where the energy is deposited. The results can be used as input parameters for the simulation of (time-dependent) temperature distributions within the layer system. These simulations allow an efficient identification of suitable process parameters for laser melting of the PEEK layer without exceeding the annealing temperature of the bearing steel. Therefore, the laser beam propagation and the spatial energy deposition in the PEEK powder are investigated in this paper.

2. Material System and Approach

2.1. Material System

The investigated material system is constituted by a cylindrical steel (∅ 31 mm) substrate and a layer of particulate PEEK powder with a thickness of approximately 50 µm. In the initial state (referred to as untreated), the steel substrates are grinded and the surface has an average roughness index of $R_a \approx 0.2$ µm. For reference measurements, the steel substrates were polished ($R_a \approx 0.01$ µm), thus the effects of surface roughness on the optical properties can be taken into account. The powder blend used for the investigations is provided by *Evonik Industries* [3] and contains PEEK particles and laser absorbers as additives for an increase of absorptivity. The average particle size of the PEEK powder is approximately 5 µm. A SEM picture of the used PEEK powder and the particle-size distribution is shown in Fig. 3. A schematic overview of the investigated material system and the interaction with the incident laser radiation is shown in Fig. 2. Due to the technique of measurement, a disk made of fused silica (UV-VIS-NIR) or potassium bromide (IR) with a thickness of 2 mm is placed on top of the PEEK layer for the spectrometric measurements.

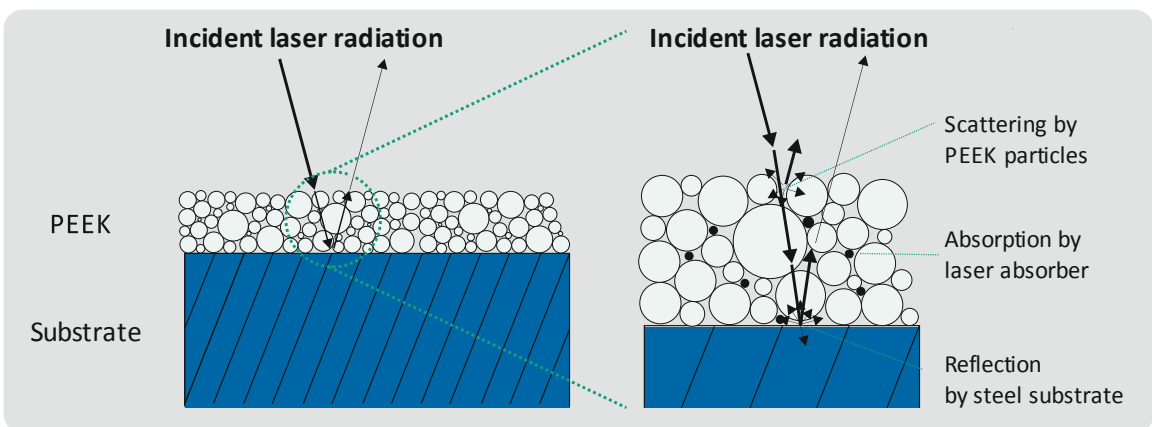

Fig. 2.: Schematic overview of the investigated material system and the interaction with the incident laser radiation.

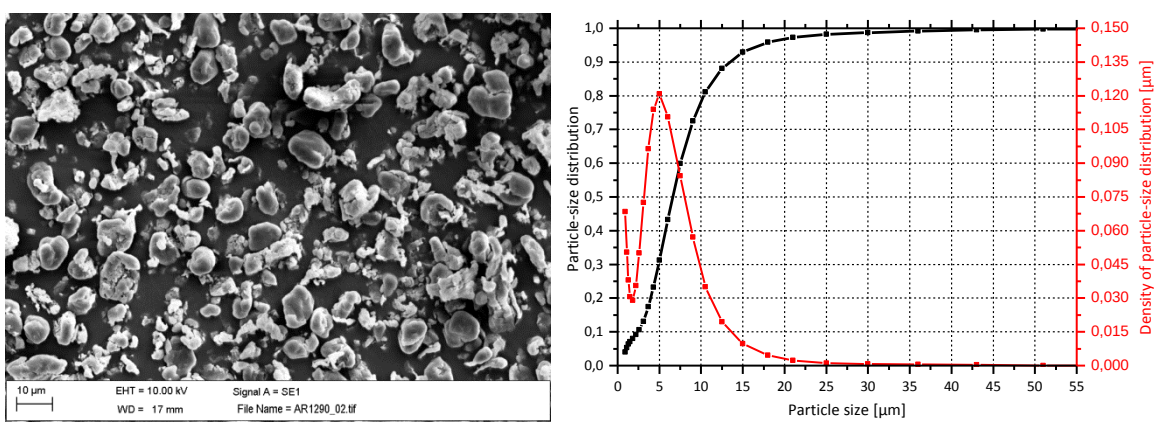

Fig. 3.: SEM picture of PEEK powder (left) and particle-size distribution (right) measured by means of laser diffraction [3].

2.2. Approach

For the investigation of the optical properties of the system consisting of steel substrate and PEEK layer, initially, the complex refractive index **n** of the bulk materials which describes refraction and absorption in an isotropic, homogeneous medium has to be extracted (Fig. 4). Therefore, the reflectance *R* and transmittance *T* of a PEEK foil, a fused silica disk, a potassium bromide disk, and polished steel substrates ($T = 0$) are measured with a double beam UV-VIS-NIR spectrometer (*Lambda 1050, PerkinElmer*) for wavelengths between 250 nm and 2500 nm and a an FTIR spectrometer (*Frontier MIR, PerkinElmer*) for wavelengths between 2500 nm and 17000 nm. In both experimental setups an integrating sphere is used to detect diffuse and directional reflected or transmitted radiation. Subsequently, a model-based simulation (see chapter 3) is conducted and fitted to the measured spectra to calculate the complex index of refraction **n** dependent on the wavelength.

Afterwards, the reflectance *R* of a layer systems consisting of steel substrate, PEEK powder and glass disk (according to spectral domain) is measured with the named spectrometers. The following parameters are investigated:

- Thickness of PEEK layer
- Ratio of laser absorber in PEEK powder
- Pre-treatment of steel substrate (polished/steel substrate)

Thereafter, the reflectance *R* of the layer systems is simulated based on different models (see chapter 3) and compared with the measured spectra.

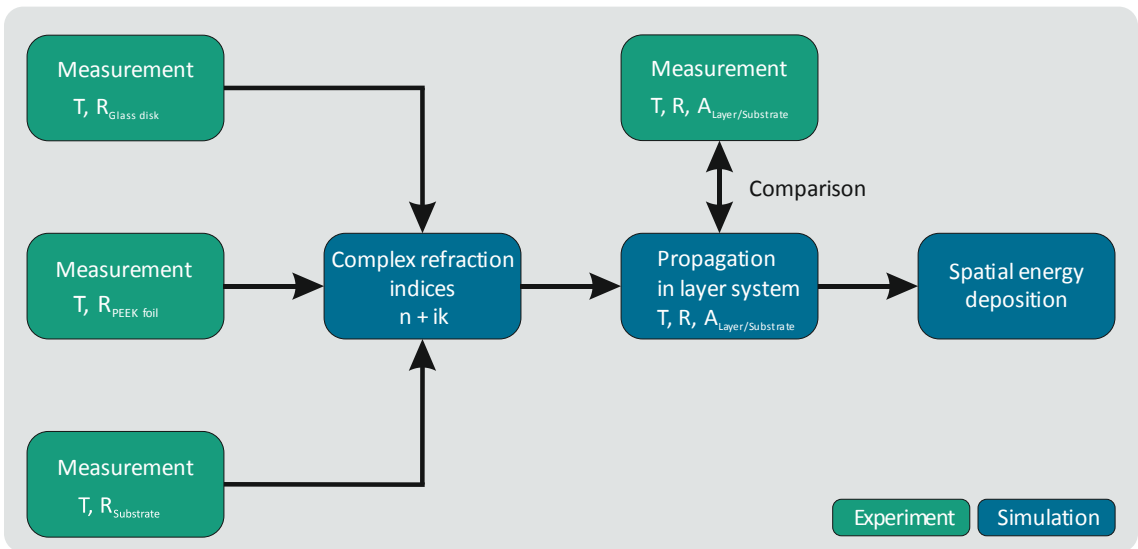

Fig. 4.: Approach for the investigation of optical properties.

3. Modelling

3.1. Complex refractive indices

The complex refractive index $\mathbf{n} = n + ik = \sqrt{\varepsilon_r}$ derives from the dielectric function $\varepsilon_r = 1 + \chi_e$ which describes the optical properties of a non-magnetic medium ($\mu_r \approx 1$). The susceptibility χ_e is defined as the constant of proportionality relating an electric field **E** to the induced dielectric polarization density **P** of a medium according to $\mathbf{P} = \varepsilon_0 \chi_e \mathbf{E}$ with ε_0 as the electric permittivity of free space. It can be described as the sum of various contributions in accordance with equation *(1)*.

$$\chi_e = \sum\nolimits_i \chi_{e,i} \qquad (1)$$

The different contributions to the susceptibility are dependent on wavelength. With the software *Scout* by *W. Theiss Hard- and Software* [4] these contributions can be calculated based on the following models:

A constant background in form of a constant complex susceptibility can often be used to describe interactions between electromagnetic radiation and matter far away from any resonances.

The Kim oscillator [5] is based on a damped harmonic oscillator and can be used to describe resonance phenomena when electromagnetic radiation interacts with matter, for example excitation of molecular vibrations. In contrast to the classical damped harmonic oscillator the Kim oscillator includes a parameter that modifies the form of the resonance curve within the extreme cases Gauss curve and Lorentz curve. The corresponding susceptibility can be described as:

$$\chi_e(\omega) = \frac{f^2}{\omega_{res}^2 - \omega^2 - i\omega\tau(\omega)}; \qquad \tau(\omega) = \gamma \exp\left(-\frac{1}{1+\sigma^2} \left(\frac{\omega_{res} - \omega}{\gamma} \right)^2 \right) \qquad (2)$$

ω_{res} : resonance frequency, f: Strenght of oscillation, γ : damping, σ : Gauss-Lorentz-Switch

The Enhanced Drude model is used to describe the behavior of free charge carrier (free electron gas) interacting with electromagnetic radiation. It differs from the simple Drude model in a frequency dependent damping. For the simple Drude model, the damping constant is given by the inverse of the mean free time of conduction electrons. The corresponding susceptibility of the enhanced model can be described as [6]:

$$\chi_e(\omega) = \frac{\omega_p^2}{\omega^2 + i\omega\gamma(\omega)}; \qquad \gamma(\omega) = \gamma_{low} - \frac{\gamma_{low} - \gamma_{high}}{\pi} \left[\tan^{-1}\left(\frac{\omega - \omega_{cross}}{\omega_{width}} \right) + \frac{\pi}{2} \right] \qquad (3)$$

ω_p : resonance frequency, $\gamma(\omega)$: frequency dempendent damping,

γ_{low} : damping constant for low frequency domain, γ_{high} : damping constant for high frequency domain,

ω_{width} : width of transitional range between low and high frequency domains, ω_{cross} : center position of transitional range

The O'Leary-Johnson-Lim (OJL) model describes interband transitions in solid state bodies where expressions for the joint density of states are given for the optical transition from the valence band to the conduction band [7]. In this model, the absorption coefficient α is described by the term $\alpha(\hbar\omega) \propto \left(\hbar\omega - E_g\right)^{1/2}$ with the energy of the band gap E_g. This term results from the simplified assumption of a parabolic form for valence and conduction band with tail states exponentially decaying into the band gap [8]. Via the Kramers-Kronig relationship [7] the real part of the dielectric function is calculated from the absorption coefficient.

In order to calculate the complex refractive index (or the dielectric function) of the bulk materials, firstly, the relevant models and initial values for the variables have to be determined. Consequently, the optical properties of the simulated material system are defined and reflectance as well as transmittance can be calculated. In a second step, the simulated spectra reflectance is fitted to the measured spectra. Once the quality of the fit is sufficient, the complex refractive indices or the dielectric function can be extracted in dependence of the wavelength.

3.2. Propagation in particulate PEEK layer

The software *Spray* from *W. Theiss Hard- and Software* [3] is used for simulating the propagation of laser radiation in the material system and for calculating the spatial energy deposition in the particulate PEEK layer. The laser beam propagation through the material system is simulated by ray tracing. The output parameters of the simulations are the reflectance, transmittance and absorbance of the considered system. The following properties of the material system were taken into account:

- calculated complex refractive indices of the bulk materials (see section 3.1)
- measured particle size distribution (Fig. 3)
- measured powder density
- measured layer thickness
- multiple reflection
- various scattering effects

The scattering effects were considered according to the theory of Mie scattering [9], an effective medium approach for porose media according to the Bruggeman modell [10], and a random interface approach. For the different scattering effects the reflectance of the layer system was simulated and compared to the measurements. Subsequently, based on the simulation results the spatial energy deposition in the layer system has been extracted for Nd:YAG laser radiation.

4. Results

4.1. Complex refractive indices

The measured and simulated reflectance spectra of polished and untreated steel substrate as well as the reflectance and transmittance spectra of a PEEK foil are exemplarily shown in Fig. 5. The graphs for the simulated spectra include the fluctuation margin of the results. In both cases the measured spectra can be described by the simulation with a sufficient accuracy. The same applies to the disks made of fused silica and potassium bromide.

As described in chapter 3, the simulation results are used to extract the complex dielectric function for the bulk materials in dependence of the wavelength. The outcome for the dielectric functions of the used steel and PEEK are shown in Fig. 6.

For the used 100Cr6 steel, there are no measured spectra available in the literature. Therefore, the results are compared to the dielectric function of pure iron [11] for the wavelengths 1000 nm and 10000 nm. The real part of the dielectric function differs from the values given in the literature by a factor of 1.4 and 1.9, respectively. The imaginary part differs by a factor of 3.3 and 1.2, respectively. These deviations are expected to arise from the difference in the composition of pure iron and 100Cr6 steel.

For PEEK, the calculated real part of the refractive index for the visible spectrum is located between n = 1.60 and n = 1.79. This is in agreement with values given in the literature (n = 1.65 – 1.79) [12].

For the fused silica disk, the real part of the refractive index (n = 1,485) deviates from the values given in the literature (n = 1,451) [13] by approximately 2.3 % for a wavelength of 1064 nm.

For the potassium bromide disk, the real part of the refractive index (n = 1,570) deviates from the values given in the literature (n = 1,527) [14] by approximately 2.8 % for a wavelength of 9724 nm.

Consequently, the measured spectra can be described be the model-based simulations and provide values for the refractive index that agree with values given in the literature. Therefore, it is assumed that the model-based simulations can be used to describe the optical properties of the bulk materials.

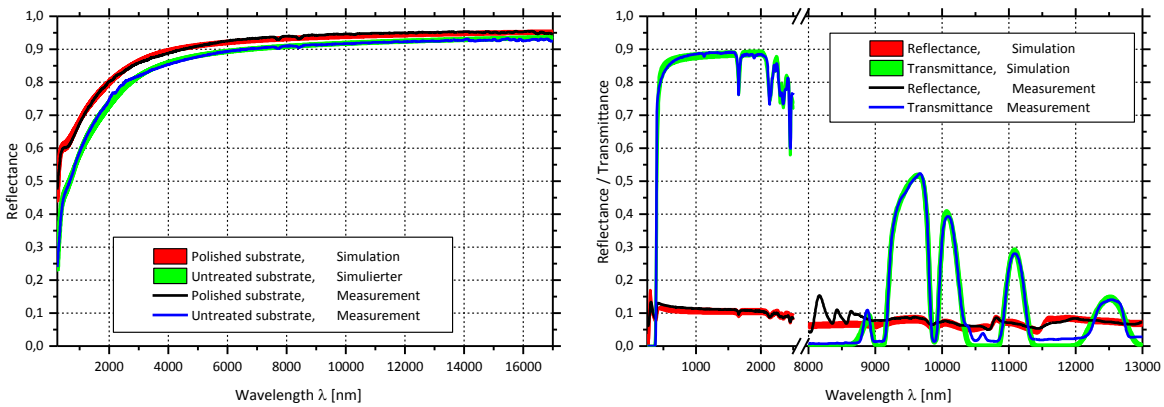

Fig. 5.: Measured and simulated reflectance and transmittance for steel substrate and PEEK foil.

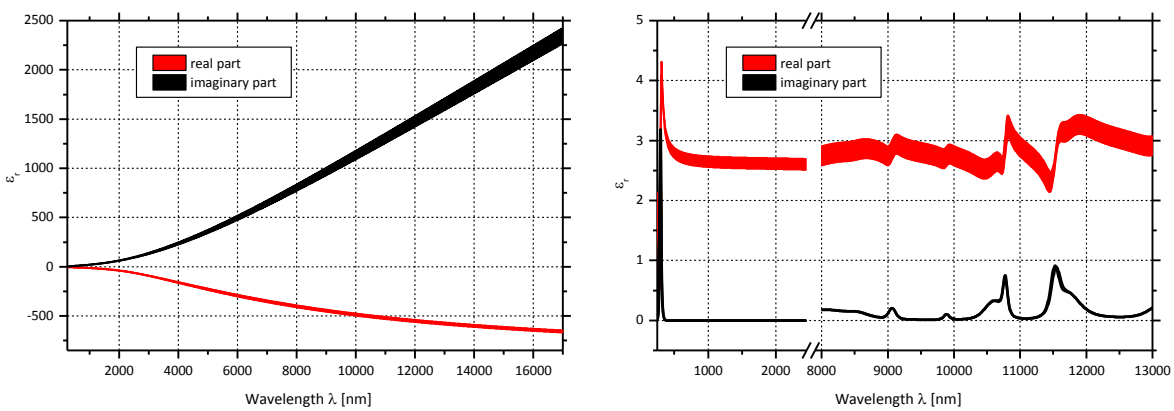

Fig. 6.: Complex dielectric function in dependence of the wavelength for steel substrate and PEEK foil.

4.2. Propagation in PEEK powder and spatial energy deposition

The simulated and measured reflectance of a material system consisting of an untreated steel substrate, a 35 µm thick particulate PEEK layer and a fused silica disk is shown in Fig. 7 for 0.1 % and 0.2 % fraction of laser absorber in the PEEK powder. The scattering effects are calculated according to the Mie-theory. In comparison to the other considered models (see section 3.2), this model generates the smallest deviation between measurements and simulation. The measured spectra can basically be described by the simulation in the domain of typical laser wavelength around 1000 nm for the case shown. Moreover, this conclusion applies for the variation of the fraction of laser absorber and the variation of layer thickness and pre-treatment of the steel substrates (surface roughness and oxidation). Hence, the developed simulations are expected to describe the propagation of laser radiation within the material system sufficiently precise.

Hence, based on these results, the spatial energy deposition is calculated for a wavelength of 1064 nm (Fig. 7). On the abscissa, the depth into the particulate PEEK layer along the surface normal is plotted. The ordinate shows the absorbed fraction of the incident radiation in arbitrary units. The correspondent incidence angle is 0° to the surface normal. Consequently, each bar shows the absorbed fraction of the incident laser radiation within a volume element with the lateral dimension of the entire layer and a z-dimension of 1 µm. For the purpose of comparison, an exponential function is fitted to the data. This describes the absorbance within homogeneous mediums according to Lambert-Beer's law. This exponential distribution does not conform to the simulated data, especially within the first 5 µm of the layer. The simulated data shows a maximum at approximately z = 6 µm. This behavior indicates a strong influence of scattering effects on the absorbance within the layer. The incident radiation is perpendicular to the volume elements when entering the layer. Thus, the path length within the first volume element is minimal. Due to scattering effects, the propagation of the radiation receives a lateral component. Thus, the path length of the radiation within each volume element increases within the first 5 µm.

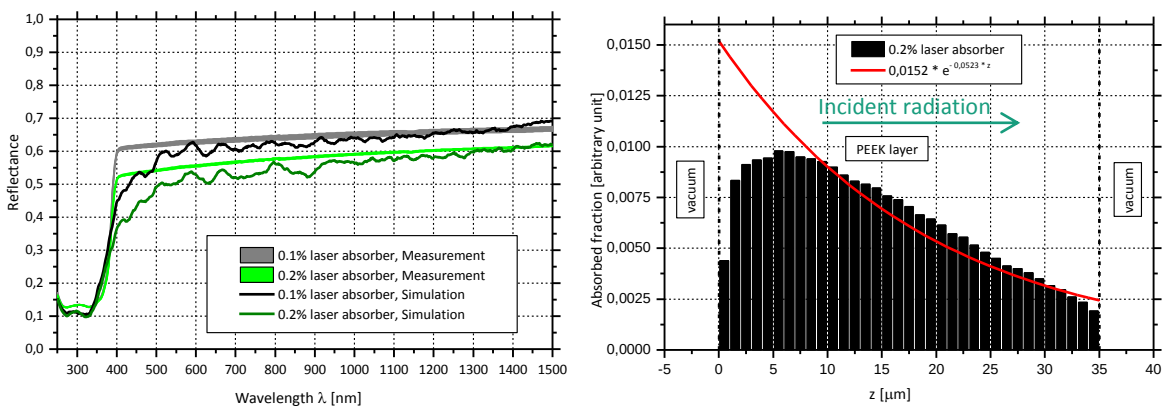

Fig. 7.: Reflectance of material system consisting of steel substrate, PEEK layer and fused silica disk (left) and spatial energy deposition within the PEEK layer for a wavelength of 1064 nm (right).

5. Conclusion

In order to simulate the propagation of laser radiation in particulate PEEK layers, initially, the reflectance and transmittance of the bulk materials are measured. Afterwards, model-based simulation is conducted and fitted to the measured data. Therefore, the complex refractive index of the bulk materials can be

calculated. Subsequently, the propagation of radiation in the layer system is simulated under the variation of properties of the layer system like layer thickness, fraction of laser absorbers and pre-treatment of the steel substrate and scattering effects. Based on this results the spatial energy deposition in the PEEK layer is extracted for Nd:YAG laser radiation.

The resulting dielectric functions and complex refractive indices conform to values given in the literature. Moreover, the measured spectra for the reflectance of layer system with a particulate PEEK layer can be described by the simulations when the scattering effects are considering according to Mie theory.

The calculated energy deposition in the particulate PEEK layer does not conform to the absorbance according to Beer–Lambert law for homogenous mediums. A maximum of the absorbed fraction along the incidence direction of the laser radiation is located approximately 6 µm under the surface of the PEEK layer. An explanation for this behavior is an increase of the path length due to scattering effects within the first 5 µm of the layer.

The next step comprises the implementation of these results into a simulation of the temperature distribution within the layer system. This leads to an efficient identification of suitable process parameters for melting the PEEK particles without exceeding the annealing temperature of the bearing steel.

Acknowledgements

The presented research was partly funded by the German Federal Ministry of Education and Research within the framework of the funding measure ‘‘Materials Innovations for Industry and Society’’ (WING). The authors would like to thank *Evonik Industries* for the measurement of the particle-size distribution of the PEEK powder and the entire consortium for the excellent cooperation within the project *Reskorr*.

References

1. Deutsche Edelstahlwerke, 2015. Data specification, Cr-legierter Wälzlagerstahl 1.3505/100Cr6
2. Domininghaus, H., 1998. Die Kunststoffe und ihre Eigenschaften Springer, 5th Edition, 978-3-54-062596-6, p. 906 ff.
3. Evonik Industries AG, Paul-Baumann-Straße 1, 45772 Marl, www.evonik.de
4. W.Theiss Hard- and Software, Dr.-Bernhard-Klein-Str. 110, DE-52078 Aachen
5. Kim, C.C., 1992. Modeling the optical dielectric function of semiconductors: Extension of the critical-point parabolic-band approximation, Physical Review B, Volume 45, Number 20
6. Drude, P., 1900. Zur Elektronentheorie der Metalle. In: Annalen der Physik. 306, Nr. 3, p. 566–613
7. Fox, M., 2001. Optical Properties of Solids, Oxford University Press, 978-0-19-850613-6, Chapter 2 & 3
8. O’Leary, S.K.; Johnson, S. R.; Lim, P. K., 1997. The relationship between the distribution of electronic states and the optical absorption spectrum of an amorphous semiconductor: An empirical analysis, Journal of Applied Physics, Vol. 82, p. 3334 – 3340
9. Mie, G., 1908, Beiträge zur Optik trüber Medien, speziell kolloidaler Metallösungen Annalen der Physik, 4. Folge, Band 25, Nr. 3, p. 377–445
10. Bruggeman, D.A.G., 1935, Berechnung verschiedener physikalischer Konstanten von heterogenen Substanzen , Annalen der Physik, 5. Folge, Band 24, p. 636–664
11. Weaver, J.H.; Krafka, C.; Lynch, D.W.; Koch, E.E.; 1981. Physics Data, Optical Properties of Metals
12. Biron, M., 2013, Thermoplastics and Thermoplastic Compositesm, William Andrew, 978-1-45-577898-0, p. 887
13. Heraeus Holding GmbH, 2015. Quarzglas für die Optik: Daten und Eigenschaften, PDF document, 30.05.2014, heraeus-quarzglas.de/media/webmedia_local/downloads/broschren_mo/SO_ Imagebroschuere_DE.pdf,
14. Korth Kristalle GmbH, 2014. Kaliumbromid, PDF document, 30.05.2014, http://www.korth.de/index.php/material-detailansicht/items/15.html?pdf=53